RESEARCH PAPER

Design and Synthesis of Novel Benzylidene-2,4-Thiazolidinedione Derivatives as PTP1B Inhibitors

Abhishek Pathak[1], Vivek Asati[2*], Naveen Gupta[1*], Ganesh Prasad Patel[1*], Brajmohan Kaushal[1*]

[1] Department of Pharmacy, Madhyanchal Professional University, Bhopal, MP, India

[2] Department of Pharmaceutical Chemistry, ISF College of Pharmacy, Moga, Punjab, India

[*] **Corresponding Authors:** Vivek Asati (Email: Vivekasatipharma47@gmail.com), Naveen Gupta, Ganesh Prasad Patel, Brajmohan Kaushal, Department of Pharmacy, Madhyanchal Professional University, Bhopal, MP, India

ABSTRACT

Protein Tyrosine Phosphatase 1B (PTP1B) is a major negative regulator of insulin and leptin signalling pathways and is an important therapeutic target for type 2 diabetes mellitus (T2DM). Ten arylidene-functionalized thiazolidine-2,4-dione (TZD) derivatives (AB1-AB10) were designed, synthesized and their characteristics were studied by the FT-IR, NMR and LC-MS analyses. In vitro testing of their PTP-1B inhibitory potential demonstrated the highest potency of compound AB1 (IC50 = 3.1 ± 0.29 µM), which was superior as compared to the reference Pioglitazone. It was also found that compounds AB9 and AB3 were also highly active with IC50 of 8.6 ± 0.37 µM and 12.25 ± 0.46 respectively. These findings were supported by molecular docking, which indicated that it strongly interacts with key residues, which include Arg47 and Phe182. In vivo experiments on STZ-NA induced diabetic mice further ensured that AB1, AB3 and AB9 were effective in reducing blood glucose levels, enhancing oral glucose tolerance, normalizing body weight and dyslipidemia. The predictions of ADMET showed excellent oral drug-likeness. Overall, the study highlights arylidene-functionalized TZD derivatives AB1, AB3 and AB9 as promising lead molecules for further development as potential therapeutic agents.

Keywords: Thiazolidinedione (TZD) derivatives; Protein Tyrosine Phosphatase 1B (PTP-1B); Type 2 Diabetes Mellitus; Enzyme inhibition; Molecular docking; ADMET prediction; Streptozotocin-nicotinamide model.

How to cite this article: Pathak A, Asati V, Gupta N, Patel GP, Kaushal B. Design and Synthesis of Novel Benzylidene-2,4-Thiazolidinedione Derivatives as PTP1B Inhibitors. Int J Drug Deliv Technol. 2026;16(23s): 806-822. DOI: 10.25258/ijddt.16.23s.86

Source of support: Nil.

Conflict of interest: None

1. INTRODUCTION

Diabetes has become one of the critical health issues that is seen as a major health threat of the 21st century. According to the International Diabetes Federation (IDF) Diabetes Atlas (10th edition, 2021), approximately 537 million adults aged 20-79 years were living with diabetes worldwide in 2021. This number is projected to increase to 783 million by 2045, underscoring the urgent need for effective therapeutic interventions, particularly in India [1, 2]. It is a long-lasting, multifactorial metabolic disease characterised by continuous hyperglycemia due to malfunctions in insulin secretion, insulin action, or both. Such metabolic imbalance impairs normal control of carbohydrates, fats and proteins that may result in severe health problems involving the eyes, kidneys, nerves, heart and blood vessels. There are three common forms of diabetes, namely Type 1 Diabetes Mellitus (T1DM), Type 2 Diabetes Mellitus (T2DM), and Gestational Diabetes Mellitus (GDM) [3-5]. Protein tyrosine phosphatase-1B (PTP-1B) serves as an important negative regulator of insulin and leptin signalling by dephosphorylating the insulin receptor and its substrates, which reduces downstream signal transduction. It is mainly found in metabolic tissues like the liver, adipose tissue, skeletal muscle, and brain, and its heightened activity is closely linked to insulin resistance, type-2 diabetes mellitus, and obesity. Blocking PTP-1B improves insulin sensitivity and glucose regulation, confirming it as a legitimate therapeutic target for metabolic conditions [6-9]. Despite the reports of various synthetic and natural PTP-1B inhibitors, their clinical advancement is

hampered by issues like poor selectivity, low bioavailability, and safety worries, which motivate continued efforts to create selective and pharmacokinetically optimized inhibitors [7, 8]. Trodusquemine (MSI-1436) and Pioglitazone are inhibitors of PTP-1B that boost insulin and leptin signalling, showing promise for treating diabetes and obesity [10, 11]. Nonetheless, natural PTP-1B inhibitors like berberine, quercetin, and chlorogenic acid face limitations due to side effects and pharmacokinetic issues [12, 13]. 2,4-thiazolidinedione (TZDs) scaffold represents a highly versatile synthetic scaffold that medicinal chemists have utilized to identify novel compounds in the target-specific approach to treat or manage various fatal diseases [14]. A 3D-QSAR study was conducted on a series of novel thiazolidinedione derivatives by self-organising molecular field analysis (SOMFA) to correlate the molecular architecture of the structure with the observed PTP-1B inhibitory activities [15]. The analysis of already published PTB-1B inhibitors (**Figure 1**) by Bhattarai et al. (2009, IC_{50} = 5.0 µM [16]; 2010, IC_{50} = 1.3 µM) [17], Wang et al. (2017, IC_{50} = 10.1 µM) [18], Hussain et al. (2019, IC_{50} = 0.98 µM) [19], and Huneif et al. (2022, IC_{50} = 15.50 µM) [20]. Guided by these structure–activity relationship (SAR) insights from earlier reports, a common pharmacophoric framework was identified and integrated to design a proposed scaffold aimed at improving PTP-1B inhibition while maintaining favorable drug-like properties. Based on these structure-activity data, the proposed scaffold was rationally constructed to combine these important pharmacophoric features to provide a high level of PTP-1B inhibitory activity.

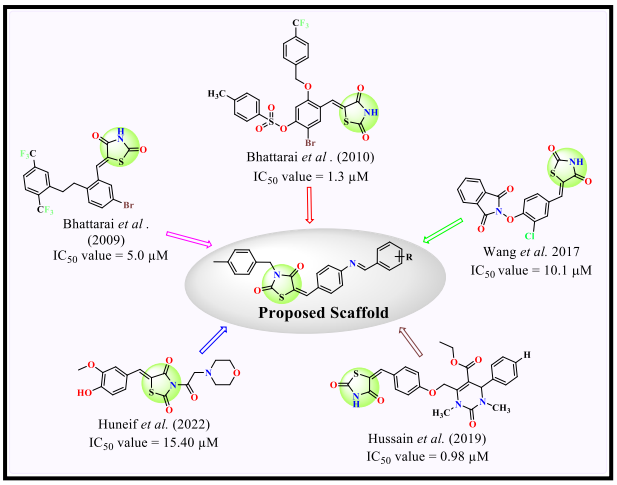

Figure 1: Literature of the proposed scaffold structure

2. MATERIAL AND METHOD

The chemicals necessary for the experimental work were purchased from various chemical suppliers, including Merck India Ltd., CDH (Central Drug House), Sigma-Aldrich, and SD Fine. The chemicals, including chloroacetic acid, thiourea, potassium carbonate, 1-(chloromethyl)-4-methylbenzene, and 4-nitrobenzaldehyde, were purchased from TCI. The solvents, such as n-hexane, acetone, isopropyl alcohol, and chloroform from Lachemie, as Well as Methanol, ethanol, HCl, glacial acetic acid from SD Fine, and other chemicals from AVRA. All the reaction were carried out in dry borosilicate glassware at room temperature or reflux assembly. Ready-made aluminium-backed TLC GF254 plates on which spot visualisations examining under a UV chamber at 360 nm. The solvents were dried and freshly distilled before use using a standard procedure. Uncorrected melting points of the compounds were measured in the open glass capillaries with a melting point apparatus. IR spectra were obtained on a Thermofischer, FT-IR spectrophotometer with the help of KBr pellets, at ISFAL in ISF College of Pharmacy, Moga (Punjab). ^{1}H NMR and ^{13}C NMR spectra were obtained from…….. A Jeol 600 MHz spectrometer was used to record proton (^{1}H) Nuclear Magnetic Resonance spectra of solutions in DMSO, and the values were given in parts per million (ppm).

Carbon Nuclear Magnetic Resonance (^{13}C NMR) were done in a Jeol at 151 MHz spectrometer on DMSO solutions, and the value was presented in parts per million (ppm). Downfield δ TMS values have been expressed in chemical shifts. The NMR signals were measured with respect to s (singlet), d (doublet), t (triplet), q (quartet), m (multiplet), and bs (broad singlet). The values of the coupling constant (J) are presented in hertz. Mass spectra were acquired using a Q-TOF Micro quadrupole time-of-flight mass spectrometer (Waters, USA) coupled to an LC-MS system and was obtained from……Punjab. The entire evaporations was done at reduced pressure on a Buchi-rotary evaporator.

2.2 General procedure for the synthesis of AB1-AB10

The proposed molecules were synthesized using Schemes 1. The thiazolidine-2,4-dione core was synthesized using methods reported in the literature. Thiazolidine-2, 4-dione derivatives (AB1-AB10) were produced by using a series of steps in the reaction. The thiazolidine-2,4-dione (3) was initially obtained by

refluxing chloroacetic acid (1) plus thiourea (2) in concentrated HCl, then cooled, and recrystallized using methanol. Attack on compound 3 by N-alkylation with 4-methylbenzyl chloride using anhydrous K_2CO_3 in the presence of solvent DMF the reaction was refluxed and later after recrystallization yields compound 5. Knoevenagel condensation of compound 5 with 4-nitrobenzaldehyde in ethanol in the presence of glacial acetic acid resulted in (Z)-5-(4-nitrobenzylidene)thiazolidine-2,4-dione (7). Reduction of the nitro group of the compound 7 was done using $SnCl_2$, HCl or catalytic hydrogenation in DMF to yield (E)-5-4-aminobenzylidene derivative (8). Lastly, compound 8 was condensed with different substituted benzaldehydes in ethanol under reflux in the presence of acetic acid catalyst to give a series of Schiff base derivatives (AB1-AB10). The purity of the compounds was evaluated through thin-layer chromatography with suitable solvent systems. Physicochemical characteristics, such as melting point, appearance, and solubility, were assessed and determined to align with the suggested structures.

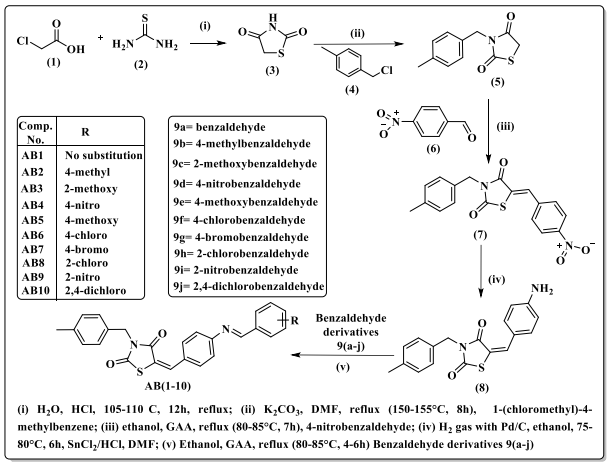

Scheme 1. Synthetic Scheme of thiazolidine-2,4-dione Synthesized Derivatives AB(1-10)

The Spectral Analysis of synthesized compounds:

1. **5-((E)-4-(((E)-benzylidene)amino)benzylidene)-3-(4-methylbenzyl)thiazolidine-2,4-dione (AB1)**

Yield: 75%, Light white, mp: 245-247 **°C**; **FT-IR (KBr, ν cm^{-1}):** 3054 (C-H, str), 2948 (C-H, alkanes), 1700 (C=O), 1654 (C=N), 1588 (C=C), 1464 (-CH_2), 1354 & 1292 (C-S), 1350 (-CH_3), 1207 (C-N), 816 (C-H, bend); **^{1}H NMR** (600 MHz, $CDCl_3$) δ 8.90 (s, 1H, N=CH), 8.25 (d, 2H, Ar-CH), 8.20 (s, 1H, TZD=CH-Ar), 7.82 (d, 2H, Ar-CH), 7.62 (t, 1H, Ar-CH), 7.44 (d, 2H, Ar-CH), 7.41 (d, 2H, Ar-CH), 7.19 (d, 2H, Ar-CH), 7.10 (d, 2H, Ar-CH), 4.83 (d, 2H, Aryl-CH_2), and 2.26 (t, 3H, Ar-CH_3); **^{13}C NMR** (151 MHz, $CDCl_3$): δ 169.30, 166.79, 160.34, 148.45, 139.94, 137.08, 136.15, 135.77, 132.49, 131.14, 131.11, 129.49, 129.49, 129.18, 129.18, 129.06, 129.06, 128.69, 128.69, 128.26, 123.76, 123.76, 111.66, 46.41, 21.42; LC/MS APCI m/z [M+H] $^+$; 413.47, Found; 412.51.

2. **3-(4-methylbenzyl)-5-((E)-4-(((E)-4-methylbenzylidene)amino)benzylidene)thiazolidine-2,4-dione (AB2)**

Yield: 69% , Green, mp: 255-257 **°C**; **FT-IR (KBr, ν cm^{-1}):** 3058 (C-H, str), 2956 (C-H, alkanes), 1723 (C=O), 1675 (C=N), 1516 (C=C), 1449 (-CH_2), 1351 & 1313 (C-S), 1487 (-CH_3), 1299 (C-N), 860 (C-H, bend); **^{1}H NMR** (600 MHz, $CDCl_3$) δ 8.90 (s, 1H, N=CH), 8.22 (s, 1H, TZD=CH-Ar), 7.69 (d, 2H, Ar-CH), 7.69 (d, 2H, Ar-CH), 7.62 (t, 1H, Ar-CH), 7.43 (d, 2H, Ar-CH), 7.28 (d, 2H, Ar-CH), 7.19 (d, 2H, Ar-CH), 7.06 (d, 2H, Ar-CH), 4.86 (d, 2H, Aryl-CH_2), 2.32 (t, 3H, Ar-CH_3) and 2.14 (t, 3H, Ar-CH_3); **^{13}C NMR** (151 MHz, $CDCl_3$): δ 169.32, 166.79, 158.40, 139.91, 138.59, 137.11, 136.15, 133.81, 132.32, 131.16, 131.16, 129.68, 129.68, 129.30, 129.30, 128.76, 128.76, 127.78, 127.78, 123.85, 123.85, 111.83, 53.29, 21.77; LC/MS APCI m/z [M+H] $^+$; 427.74, Found; 426.53.

5-((E)-4-(((E)-2-methoxybenzylidene)amino)benzylidene)-3-(4-methylbenzyl) thiazolidine-2,4-dione (AB3)

Yield: 74% , Light white, mp: 275-277 **°C**; **FT-IR (KBr, ν cm^{-1}):** 3104 (C-H, str), 2864 (C-H, alkanes), 1721 (C=O), 1661 (C=N), 1583 (C=C), 1484 (-CH_2), 1350 & 1320 (C-S), 1383 (-CH_3), 1247 (C-N), 1161 (C-O-C), and 861 (C-H, bend); **^{1}H NMR** (600 MHz, $CDCl_3$) δ 8.89 (s, 1H, N=CH), 8.17 (s, 1H, TZD=CH-Ar), 7.84 (d, 1H, Ar-CH), 7.75 (d, 2H, Ar-CH), 7.61 (t, 1H, Ar-CH), 7.36 (d, 2H, Ar-CH), 7.28 (t, 1H, Ar-CH), 7.18 (d, 2H, Ar-CH), 7.13 (d, 1H, Ar-CH), 7.09 (d, 2H, Ar-CH), 4.85 (d, 2H, Aryl-CH_2), 3.91 (t, 3H, O-CH_3) and 2.26 (t, 3H, Ar-CH_3); **^{13}C NMR** (151 MHz, $CDCl_3$): δ 169.24, 166.84, 159.58, 156.56, 148.13, 139.91, 137.11, 136.15, 132.32, 131.19, 131.19, 130.37, 129.68, 129.68, 129.30, 129.30, 127.48, 124.96, 123.78, 123.78, 119.89, 111.83, 111.19, 55.64, 46.57, 21.77; LC/MS APCI m/z [M+H] $^+$; 443.30, Found; 442.53.

3. **3-(4-methylbenzyl)-5-((E)-4-(((E)-4-nitrobenzylidene)amino)benzylidene)thiazolidine-2,4-dione (AB4)**

Yield: 72%, yellowish green, mp: 252-254 **°C**; **FT-IR (KBr, ν cm^{-1}):** 3086 (C-H, str), 2936 (C-H, alkanes),

1721 (C=O), 1648 (C=N), 1589 (C=C), 1549 & 1343 (-NO_2), 1453 (-CH_2), 1332 & 1300 (C-S), 1421 (-CH_3), 1253 (C-N), 860 (C-H, bend); **^{1}H NMR** (600 MHz, $CDCl_3$) δ 9.14 (s, 1H, N=CH), 8.35 (s, 1H, TZD=CH-Ar), 8.08 (d, 2H, Ar-CH), 7.91 (d, 2H, Ar-CH), 7.80 (d, 2H, Ar-CH), 7.52 (d, 2H, Ar-CH), 7.18 (d, 2H, Ar-CH), 7.08 (d, 2H, Ar-CH), 4.83 (d, 2H, Aryl-CH_2), and 2.25 (t, 3H, Ar-CH_3); **^{13}C NMR** (151 MHz, $CDCl_3$): δ 169.32, 166.79, 158.40, 150.16, 147.08, 139.91, 137.11, 136.15, 133.81, 132.32, 131.19, 131.19, 130.32, 130.32, 129.68, 129.68, 129.30, 129.30, 124.31, 124.31, 123.85, 123.85, 111.83, 46.57, 21.77; LC/MS APCI m/z [M+H] $^+$; 458.18, Found; 457.50.

5-((E)-4-(((E)-4-methoxybenzylidene)amino)benzylidene)-3-(4-methylbenzyl)thiazolidine -2,4-dione (AB5)

Yield: 78% , Light white, mp: 225-227 **°C**; **FT-IR (KBr, ν cm^{-1}):** 3075 (C-H, str), 2931 (C-H, alkanes), 1702 (C=O), 1682 (C=N), 1591 (C=C), 1471 (-CH_2), 1368 & 1341 (C-S), 1441 (-CH_3), 1232 (C-N), 1202 (C-O-C), and 771 (C-H, bend); **^{1}H NMR** (600 MHz, $CDCl_3$) δ 8.82 (s, 1H, N=CH), 8.17 (s, 1H, TZD=CH-Ar), 7.80 (d, 2H, Ar-CH), 7.64 (d, 2H, Ar-CH), 7.33 (d, 2H, Ar-CH), 7.18 (d, 2H, Ar-CH), 7.14 (t, 2H, Ar-CH), 7.08 (d, 2H, Ar-CH), 4.80 (d, 2H, Aryl-CH_2), 3.89 (t, 3H, O-CH_3) and 2.27 (t, 3H, Ar-CH_3); **^{13}C NMR** (151 MHz, $CDCl_3$): δ 168.98, 166.57, 159.84, 157.93, 148.58, 140.27, 137.53, 136.46, 132.24, 131.49, 131.49, 131.16, 131.19, 130.28, 129.68, 129.68, 129.30, 129.30, 123.78, 123.78, 114.84, 114.84, 111.44, 55.78, 46.37, 21.32; LC/MS APCI m/z [M+H] $^+$; 443.55, Found 442.53.

6. 5-((E)-4-(((E)-4-chlorobenzylidene)amino)benzylidene)-3-(4-methylbenzyl)thiazolidine-2,4-dione (AB6)

Yield: 78% , Greyish, mp: 259-261 **°C**; **FT-IR (KBr, ν cm^{-1}):** 3058 (C-H, str), 2985 (C-H, alkanes), 1705 (C=O), 1654 (C=N), 1511 (C=C), 1492 (-CH_2), 1315 & 1292 (C-S), 1387 (-CH_3), 1208 (C-N), 839 (C-H, bend) and 542 (C-Cl); **^{1}H NMR** (600 MHz, $CDCl_3$) δ 8.89 (s, 1H, N=CH), 8.22 (s, 1H, TZD=CH-Ar), 7.89 (d, 2H, Ar-CH), 7.49 (d, 2H, Ar-CH), 7.46 (d, 2H, Ar-CH), 7.44 (d, 2H, Ar-CH), 7.18 (d, 2H, Ar-CH), 7.08 (d, 2H, Ar-CH), 4.85 (d, 2H, Aryl-CH_2), and 2.26 (t, 3H, Ar-CH_3); **^{13}C NMR** (151 MHz, $CDCl_3$): δ 169.19, 166.77, 158.27, 148.78, 139.87, 137.24, 136.24, 134.65, 134.19, 132.68, 131.16, 131.16, 130.28, 130.28, 129.68, 129.68, 129.30, 129.30, 129.07, 129.07, 123.78, 123.78, 11.67, 46.32, 21.60; LC/MS APCI m/z [M+H] $^+$; 447.11, Found; 446.95.

7. 5-((E)-4-(((E)-4-bromobenzylidene)amino)benzylidene)-3-(4-methylbenzyl)thiazolidine-2,4-dione (AB7)

Yield: 85% , Brown, mp: 234-236 **°C**; **FT-IR (KBr, ν cm^{-1}):** 3068 (C-H, str), 2914 (C-H, alkanes), 1717 (C=O), 1655 (C=N), 1527 (C=C), 1481 (-CH_2), 1350 & 1245 (C-S), 1387 (-CH_3), 1285 (C-N), 825 (C-H, bend) and 508 (C-Br); **^{1}H NMR** (600 MHz, $CDCl_3$) δ 8.84 (s, 1H, N=CH), 8.18 (s, 1H, TZD=CH-Ar), 7.88 (d, 2H, Ar-CH), 7.78 (d, 2H, Ar-CH), 7.51 (d, 2H, Ar-CH), 7.37 (d, 2H, Ar-CH), 7.18 (d, 2H, Ar-CH), 7.08 (d, 2H, Ar-CH), 4.85 (d, Aryl-CH_2), and 2.25 (t, 3H, Ar-CH_3); **^{13}C NMR** (151 MHz, $CDCl_3$): δ 169.47, 166.90, 158.11, 148.27, 139.97, 137.38, 136.13, 135.25, 132.68, 131.95, 131.95, 131.16, 131.16, 129.30, 129.30, 129.07, 129.07, 128.64, 128.64, 123.78, 123.78, 122.32, 111.23, 46.24, 21.11; LC/MS APCI m/z [M+H] $^+$; 492.55, Found; 491.40.

8. 5-((E)-4-(((E)-2-chlorobenzylidene)amino)benzylidene)-3-(4-methylbenzyl)thiazolidine-2,4-dione (AB8)

Yield: 71 % , Light black, mp: 285-287 **°C**; **FT-IR (KBr, ν cm^{-1}):** 3053 (C-H, str), 2922 (C-H, alkanes), 1715 (C=O), 1654 (C=N), 1522 (C=C), 1462 (-CH_2), 1374 & 1238 (C-S), 1385 (-CH_3), 1222 (C-N), 839 (C-H, bend) and 542 (C-Cl); **^{1}H NMR** (600 MHz, $CDCl_3$) δ 9.09 (s, 1H, N=CH), 8.28 (s, 1H, TZD=CH-Ar), 7.88 (d, 1H, Ar-CH), 7.80 (d, 2H, Ar-CH), 7.55 (t, 1H, Ar-CH), 7.52 (d, 1H, Ar-CH), 7.47 (t, 1H, Ar-CH), 7.41 (d, 2H, Ar-CH), 7.18 (d, 2H, Ar-CH), 7.08 (d, 2H, Ar-CH), 4.84 (d, 2H, Aryl-CH_2), and 2.24 (t, 3H, Ar-CH_3); **^{13}C NMR** (151 MHz, $CDCl_3$): δ 169.15, 166.65, 157.43, 148.53, 139.64, 137.28, 136.24, 136.24, 133.43, 132.56, 131.59, 131.19, 131.19, 130.25, 129.30, 129.30, 129.07, 129.07, 128.64, 128.64, 127.11, 123.78, 123.78, 111.55, 46.41, 21.63; LC/MS APCI m/z [M+H] $^+$; 447.76, Found; 446.95.

9. 3-(4-methylbenzyl)-5-((E)-4-(((E)-2-nitrobenzylidene)amino)benzylidene)thiazolidine-2,4-dione (AB9)

Yield: 66% , Light brown, mp: 265-267 **°C**; **FT-IR (KBr, ν cm^{-1}):** 3098 (C-H, str), 2988 (C-H, alkanes), 1708 (C=O), 1655 (C=N), 1545 (C=C), 1535 & 1355 (-NO_2), 1480 (-CH_2), 1325 & 1208 (C-S), 1388 (-CH_3), 1093 (C-N), 839 (C-H, bend); **^{1}H NMR** (600 MHz, $CDCl_3$) δ 9.33 (s, 1H, N=CH), 8.14 (d, 2H, Ar-CH), 8.10 (t, 1H, Ar-CH), 8.07 (d, 1H, Ar-CH), 8.02 (s, 1H, TZD=CH-Ar), 7.89 (d, 2H, Ar-CH), 7.81 (t, 1H, Ar-

CH), 7.54 (d, 2H, Ar-CH), 7.18 (d, 2H, Ar-CH), 7.08 (d, 2H, Ar-CH), 4.82 (d, 2H, Aryl-CH_2), and 2.35 (t, 3H, Ar-CH_3); **^{13}C NMR** (151 MHz, $CDCl_3$): δ 169.13, 166.34, 153.79, 149.26, 148.56, 139.72, 137.37, 136.38, 133.47, 132.80, 131.46, 131.19, 131.19, 129.51, 129.30, 129.30, 129.07, 129.07, 128.40, 124.39, 123.78, 123.78, 111.70, 46.32, 21.60; LC/MS APCI m/z $[M+H]^+$; 458.74, Found; 457.50.

10. 5-((E)-4-(((E)-2,4-dichlorobenzylidene)amino)benzylidene)-3-(4-methylbenzyl) thiazolidine -2,4-dione (AB10)

Yield: 52% , Light white, mp: 277-279 **°C**; **FT-IR (KBr, ν cm^{-1}):** 3052 (C-H, str), 2919 (C-H, alkanes), 1708 (C=O), 1688 (C=N), 1593 (C=C), 1464 (-CH_2), 1351 & 1226 (C-S), 1383 (-CH_3), 1108 (C-N), 824 (C-H, bend) and 521 (C-Cl); **^{1}H NMR** (600 MHz, $CDCl_3$) δ 8.93 (s, 1H, N=CH), 8.21 (s, 1H, TZD=CH-Ar), 7.81 (d, 2H, Ar-CH), 7.72 (d, 1H, Ar-CH), 7.41 (d, 2H, Ar-CH), 7.35 (t, 1H, Ar-CH), 7.29 (s, 1H, Ar-CH), 7.18 (d, 2H, Ar-CH), 7.08 (d, 2H, Ar-CH), 4.84 (d, 2H, Aryl-CH_2), and 2.24 (t, 3H, Ar-CH_3); **^{13}C NMR** (151 MHz, $CDCl_3$): δ 169.40, 166.54, 157.72, 148.31, 139.40, 137.12, 136.18, 134.80, 134.80, 133.35, 132.31, 131.16, 131.16, 129.62, 129.30, 129.30, 129.07, 129.07, 128.36, 127.53, 123.78, 123.78, 111.21, 46.72, 21.30; LC/MS APCI m/z $[M+H]^+$; 482.87, Found; 481.36.

2.3. Biological activity

The inhibitory potential of compounds AB1-AB10 on the Protein Tyrosine Phosphatase 1B (PTP1B) activity was measured by the PTP1B Inhibitor Screening Assay Kit (ab139465, Abcam) [21, 22]. The principle of the assay is a colourimetric readout, which determines the level of free phosphate that is liberated by a phosphopeptide substrate by means of the Red Assay Reagent, which comprises Malachite Green. All the reactions were done in a 96-well clear flat-bottom microplate. A microplate reader was used to determine the absorbance at 620 nm. To start the assay, 35 µL of 1X PTP1B Assay Buffer was placed into every well of a pre-warmed plate. In test wells, 10 µL of varying concentrations of each compound AB1-AB10 were put in the test wells, whereas in control wells, 10 µL of 1X Assay Buffer was put instead of the inhibitor. This was followed by 5 µL PTP1B enzyme (usually 2.5 µg/well) in all the wells. "The reaction was initiated by adding 50 µL of pre-warmed 2× PTP1B substrate solution to achieve the desired final concentration [23, 24].

2.3.2. *In vivo* parameters

2.3.2.1. Animal ethics

Anti-hyperglycemic effect of compounds AB1-AB10 was performed by the streptozotocin-nicotinamide (STZ-NA) model of the induced diabetic mice. As a reference, Pioglitazone was utilized. In an in vivo anti-hyperglycaemic study, male Swiss Albino mice with a body weight of 25+5 g and aged 8-10 weeks were used. Mice were taken from the Central Animal House Facility, ISF College of Pharmacy, G.T. Road, Ghal Kalan, Moga approved under the Institutional Animal Ethics Committee (IAEC) (ISFCP/IAEC/CPCSEA/ Meeting No.: 01/2022/Protocol No. 15). Mice in this experiment were divided and placed under the condition of pathogen free environment in which they had access to unlimited food and water and kept in control conditioned temperature at 24±2ºC on a 12 h light/12 h darkness cycle and the relative humidity was at 55-60 %.

4.3.2.2. Chemicals

Streptozotacin (STZ) was procured from Sigma-Aldrich. Nicotinamide was bought from Himedia, Mumbai, India. The anti-hyperglycemic activity of the synthesized molecules was done using glucometer and Blood glucose test strips (Alere G1 blood glucose monitoring system). STZ was suspended in 0.1 M citrate buffer (pH 4.5), and NA in normal physiological saline. The estimation of total cholesterol, triglycerides of Accurex Biomedical Ltd, and HDL-Cholesterol of Coral Clinical Systems have been done using the commercial diagnostic kits. The rest of the chemicals and reagents were of analytical grade.

6.7.2. Preparation of Drug and Dose

The dose of 20 mg/kg of body weight of compound AB1, AB9, and AB3 (orally as a suspension in carboxy methyl cellulose (CMC) (0.5 per cent w/v in water) was used. As a reference standard Pioglitazone (dose: 20 mg/kg of body weight, orally, as a suspension in carboxy methyl cellulose (CMC) was used orally as a suspension in carboxy methyl cellulose (CMC) (0.5 per cent w/v [25].

4.3.2.3. Induction of Diabetes in Albino Mice:

At first, the mice are named using their common names, as at **Table 4.2**. Mice were separated into two groups; a normal group and a diabetic group. Streptozotocin (STZ) (55mg/kg, i.p) in buffer (pH 4.5) was administered to the mice 15 minutes after nicotinamide (110mg/kg, i.p.) in normal saline induced T2DM. A blood glucose higher than 200 mg/dl can be referred to as diabetes. Hence, blood samples were taken after 72 h of STZ administration from the tail vein of the mice and

the glucose level was measured through a glucometer (Morepen glucometer). The mice whose blood glucose exceeded 230 mg/dL were regarded as diabetic and were included in the study further. Once T2DM was confirmed, mice were selected at random into normal, standard, diabetic and treatment groups (n= 6). The synthesized compound was administered orally to the treatment group at a dose of 10 mg/kg for 15 days. An equivalent volume of vehicle alone was administered to the normal and diabetic control groups. The day of first dose administration was considered as day 0 of treatment. Upon completion of the experimental protocol, multiple parameters were evaluated. Blood samples were taken by the retro-orbital plexus of the eye under ether anaesthesia [26, 27]

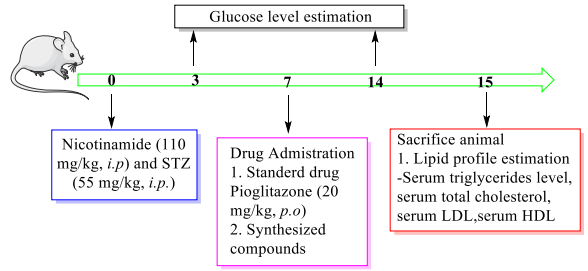

Note: One animal from each group will be sacrificed to accomplish IM analysis. Remaining mice will be return for reuse

Table 1: Experimental Analysis of Animals

S. No	Groups	Animal species	No. of animals
1	Normal Control Group	Swiss Albino Mice	6
2	Diabetic control (STZ 55mg/kg, i.p.) and Nicotinamide 110mg/kg, i.p.)		6
3	Standard drug (Pioglitazone,20mg/100 g body weight, p.o.)		6
4	Synthesized compounds AB1 (20 mg/kg, p.o.)		6
5	AB9 (20 mg/kg, p.o.)		6
6	AB3 (20 mg/kg, p.o.)		6

2.3.2.4. Statistical analysis

The statistical analysis of all results was performed with the help of GraphPad Prism version 8.0 (GraphPad Software, Inc., La Jolla, CA, United States) and provided in means and standard deviation (SD). One-way ANOVA and two-tailed ANOVA were used to analyse the results, and post hoc tests were conducted using Tukey and Bonferroni, respectively. When the $P <$ 0.01, the values were viewed as significant. All values are expressed as mean ± SD, with six animals per group (n = 6). The one-way ANOVA was used to analyse data, followed by the Newman-Keuls multiple comparison test, although the values are also presented using means and SD with n = 6. The two-way ANOVA was used to analyse data, and the Bonferroni post hoc test, $^{a}p < 0.05$, versus normal group, $^{b}p < 0.05$, versus diabetic group, $^{c}p < 0.05$, versus standard group. All the statistical analyses were performed using GraphPad Prism software $P < 0.05$ was deemed significant [28-30].

4.3.2.5. Body weight

Experimental animal models were made, and the weight of the animals was determined using a weighing machine every week or after a span of two weeks. Measurement of the weight of the animals was between 10:00 am and 11:00 am.

4.3.2.6. Blood glucose level

On a biweekly basis, each group of animals were followed until a fasting serum glucose level was taken with the help of a Touch Select glucometer (Johnson, Milpitas, CA). The measurement of the fasting glucose levels was done in the morning between the time 9:00 am to 10:00 am when the mice were fasting.

4.3.2.7. Oral Glucose Tolerance Test

The diagnosis of glucose intolerance and T2DM was done by the Oral glucose tolerance test; the test involves the overnight fasting of the animals before the test. The animals were injected with glucose (2g/kg, ip, in saline). Sampling from the tip of the tail was performed, and measurements were taken at 0, 30, 60, and 120 minutes after the bolus using the glucometer. The region under the concentration-versus-time curve (AUC glucose 0-120 min, mg/dL × minutes) was determined [31, 32].

4.3.2.8. Determination of total cholesterol, triglycerides, HDL, and LDL levels

The colourimetric method was used to reduce the levels of total cholesterol, triglycerides, LDL and HDL using a commercial assay kit, called Accurex, using a serum sample. In brief, the blood sample collected was centrifuged at a rate of 10000 rpm for 60 min at 4ºC, and the separated plasma was collected. The determination of the total cholesterol, triglycerides, HDL, and LDL levels was then done using the supernatant serum. 0.1 mL of the supernatant serum, 1 mL of the prepared working reagent and 0.1 mL of standard solutions were combined and allowed to incubate at 37ºC over a period of 60 min. At 510 nm,

the absorbance was recorded against the blank solution [33, 34].

HDL Cholesterol/Total cholesterol/total glycerides(mg/dL) = Abs. $_{Test}$/Abs. $_{Standard}$ × 25 × 2

LDL cholesterol (mg/dl) = (Total cholesterol) – (Triglycerides/5) – (HDL cholesterol)

4.4 Molecular Docking studies

The ligand molecules designed were docked into cavity number 1 of PTP-1B, which co-crystallized with ligand Pioglitazone. MolDock Score is a grid-based scoring method that was chosen at 0.3 Å grid resolutions to score the docking solutions. MolDock Simplex Evolution (MolDock SE) search algorithm, having a number of runs equal to 10 and population size equal to 50, was chosen as part of the molecular docking searches. The run specifies the number of times the docking simulation was repeated on each ligand, and the output of each repetition was one final solution, i.e., pose. The docking parameters included a maximum of 1,500 iterations, an energy threshold of 100, a binding radius of 15 Å, a maximum of 300 steps for the simplex evolution (SE) algorithm, and an SE neighbouring distance factor of 1.00. In similar poses of clusters (when multiple cluster poses are taken), the RMSD value was set to 1.00 Å. Each of them returned only the negative, lowest-energy representative cluster on completion of docking, and similarly, poses were removed, retaining the best-scoring one. The ranking of the clusters was done based on the conformations of the lowest binding energy in each group. The pose or conformation of the ligand that had the largest MolDock score was chosen to study its binding interactions with the target [35-37].

***In silico* ADME properties**

The prediction of the physicochemical properties of the acquired hits was done using *in silico* prediction after docking investigations were done using the Schrodinger Qikprop module. The parameters that were predicted were molecular weight (M.Wt), the number of hydrogen bond donors (HBD), acceptors (HBA), the octanol/water partition coefficient (log P), the expected apparent Caco-2 cell permeability in nm/sec (P Caco) and the number of rotatable bonds (Rot) (QikProp De Schrodinger Release) [38, 39].

3. Results and discussion

3.1 Chemistry

Using a multistep synthesis process, ten TZD-based derivatives AB(1-10) were synthesized in this study. The pathway started with the cyclization of chloroacetic acid and thiourea in ethanol and glacial acetic acid under reflux, yielding thiazolidine-2,4-dione. This intermediate was subsequently N-arylated with substituted aryl bromides using K_2CO_3 and DMF as the solvent under reflux to yield aryl-substituted TZD derivatives AB(1-10). The intermediates were subsequently reacted with nitrobenzaldehydes in ethanol and glacial acetic acid under reflux to introduce the nitro-substituted arylidene groups. The produced nitro groups were converted to the corresponding primary amines through either catalytic hydrogenation (H_2/Pd-C in ethanol) or by using $SnCl_2$/HCl in DMF. Finally, the amino derivatives underwent condensation with substituted benzaldehydes in ethanol and acetic acid under reflux, resulting in the desired Schiff bases containing an imine (C=N) functional group. This synthetic plan, in general, is a methodical and general technique that employs cyclization, N-arylation, nitro-functionalization, reduction, and the formation of Schiff bases to produce heterocycles of the TZD-type, covering wide structural variations. TLC was used to monitor the progress of the reaction. The TLC plates were viewed under UV chamber. Various work-up processes were used in order to purify the products of the reaction in order to eliminate unreacted starting material and impurities. To obtain pure samples of the title compounds, recrystallisation was done in appropriate solvents. Melting points and Rf values of all the intermediates and the final compounds were ascertained (Table 1). Physicochemical characterization was used to validate the structure of different compounds that were synthesized.

Description of physical or chemical properties

The masses of the synthesized compounds were in the range of the Lipinski rule of five. Table 1 displays the molecular weight, Rf value and melting points of compounds produced synthetically. The percent yield of all the compounds is good, which suggests the appropriateness of the synthetic procedures. Other compounds like AB8, AB4, AB3, AB1, AB6, AB5, AB6 and AB7 were shown to have high yield (71-85%) as compared to the series of AB2, AB9 and AB10.

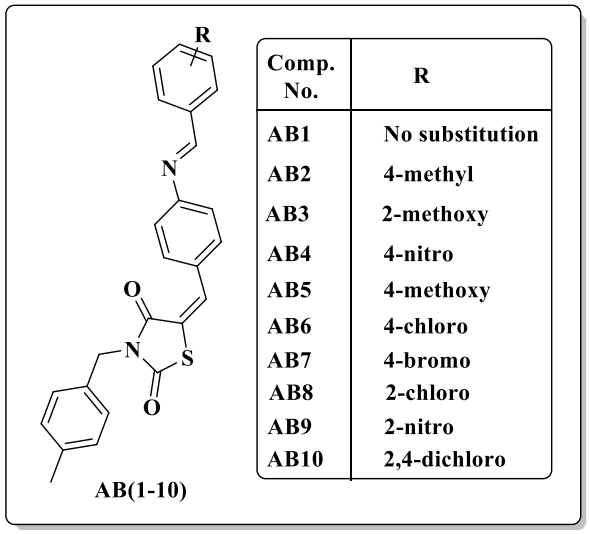

Comp. No.	R
AB1	No substitution
AB2	4-methyl
AB3	2-methoxy
AB4	4-nitro
AB5	4-methoxy
AB6	4-chloro
AB7	4-bromo
AB8	2-chloro
AB9	2-nitro
AB10	2,4-dichloro

Figure 2. Substituted arylidene TZD pharmacophore

Table 2. Physicochemical characteristics of the final compound **AB(1-10)**

Comp.	Mol. formula	Mol. wt.	Colour	M.P (°C)	R_f	%yield
AB1	$C_{25}H_{20}N_2O_2S$	412.51	Light white	245-247	0.7	75
AB2	$C_{26}H_{22}N_2O_2S$	426.53	Green	255-257	0.8	69
AB3	$C_{26}H_{22}N_2O_3S$	442.53	Light white	275-277	0.6	74
AB4	$C_{25}H_{19}N_3O_4S$	457.50	Yellowish green	252-254	0.7	72
AB5	$C_{26}H_{22}N_2O_3S$	442.53	Light white	225-227	0.6	78
AB6	$C_{25}H_{19}ClN_2O_2S$	446.95	Greyish	259-261	0.8	78
AB7	$C_{25}H_{19}BrN_2O_2S$	491.40	Brown	234-236	0.6	85
AB8	$C_{25}H_{19}ClN_2O_2S$	446.95	Light black	285-287	0.6	71
AB9	$C_{25}H_{19}N_3O_4S$	457.50	Light brown	265-267	0.5	66
AB10	$C_{25}H_{18}Cl_2N_2O_2S$	481.39	Light white	277-279	0.8	52

Description of the Spectral Analysis:

A series of novel thiazolidinedione (TZD) analogs were prepared by condensing substituted aromatic aldehydes with aminomethyl-substituted TZD to produce an arylidene-linked heterocycle with possible biological activity. All compounds AB(1-10) were structurally confirmed by details obtained from ^1H and ^{13}C NMR spectral analysis, which invariably found characteristic signals of the arylidene proton (δ 8.2-8.7 ppm), aromatic systems (δ 6.7-8. 0 ppm), methylene bridges (δ 4.5-4.9 ppm), and substituent specific methyl/methoxy protons (δ 2.1-4.0 ppm) and the presence of carbon resonances in the electronic substituents on the aryl rings could be varied to investigate structure-property relations, and the overall effect of electron-withdrawing groups on the NMR spectrum is to tend to shift the NMR spectrum downfield, as a result of deshielding. Among the synthesized analogues, compound AB1 exhibited the most favourable physicochemical properties and the highest biological activity, which can be attributed to the presence of strong electron-withdrawing substituents. These findings suggest that AB1 represents a promising lead compound and warrants further detailed pharmacological investigation.

3.4. Biological activity

3.4.1. *In vitro* PTB-1B inhibitory activity assay

Ten derivatives of aromatic aldehydes that underwent condensation with 5-amino-thiazolidine-2,4-dione to create arylidene-substituted thiazolidine-2,4-dione AB(1-10) were produced. The compounds were biologically tested based on their inhibitory effect on protein tyrosine phosphatase 1B (PTP-1B), and it was shown that some of the derivatives had a strong enzyme

inhibitory effect. The most potent of them was compound AB1, which exhibited an IC_{50} of 3.1 ± 0.29 µM, which was greater than that of the standard inhibitor Pioglitazone (IC_{50} = 11.5 ± 0.65 µM). This increased activity can be explained by the electronic and steric effects that are contributed by the aryl substituents, which might guide an intense activity in the PTP1B active site. Other active compounds were AB9 (IC_{50} = 8.54 ± 0.36 µM), AB3 (IC_{50} =12.25 ± 0.46 µM), and again, the patterns of aryl substitution were useful in modulating a biological response.

Table 3: Structure of various synthesised thiazolidine-2,4-dione derivatives AB(1-10) and their IC_{50} value

S. No.	Compound Name	Compound Structure	PTB1b inhibition (IC_{50} ± SD) µM IC_{50} value
1	**AB1**	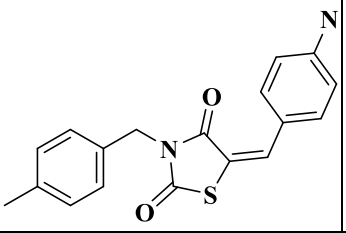	**3.1 ± 0.29**
2	**AB2**	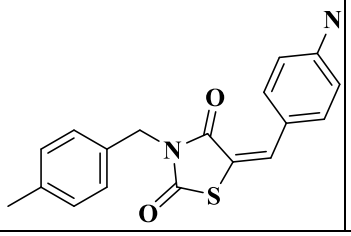	67.15 ± 0.10
3	**AB3**	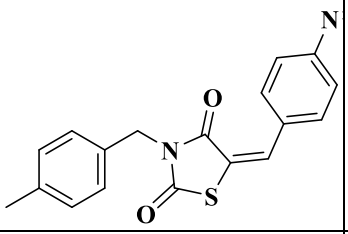	12.25 ± 0.46
4	**AB4**	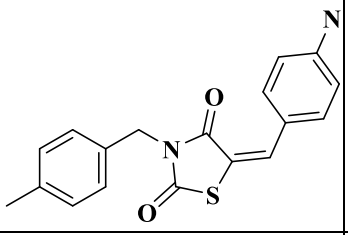	112 ± 015
5	**AB5**	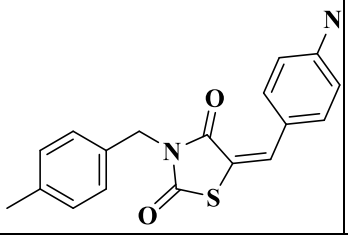	28.4 ± 0.34
6	**AB6**	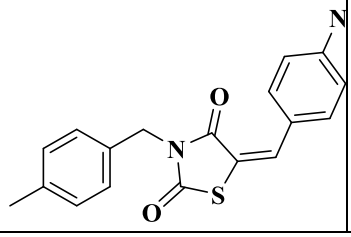	87.2 ± 0.55

7	AB7	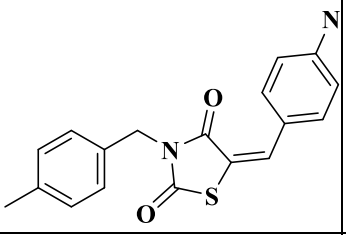	52.28 ± 0.31
8	AB8	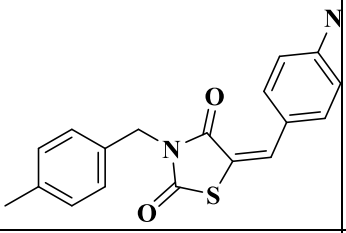	45.3 ± 0.54
9	AB9	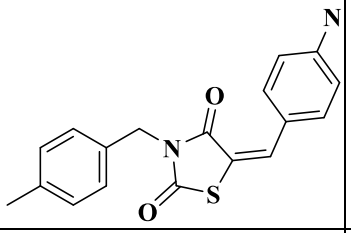	8.6 ± 0.37
10	AB10	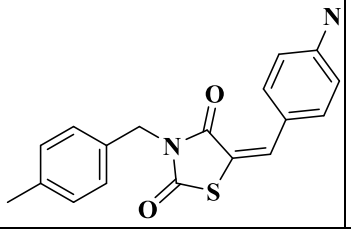	130.39 ± 0.29
11	Pioglitazone	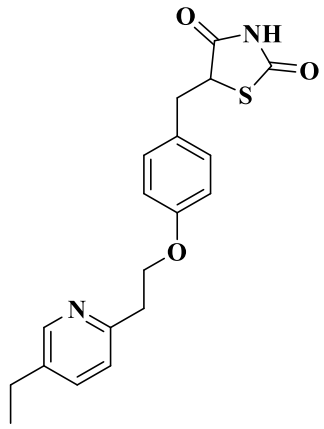	11.5± 0.65

3.4.2. In vivo studies

5.4.1 Body Weight

The study findings represented that the decrease in body weight was amazingly noted in the diabetic group relative to the normal group ($p < 0.0001$). Moreover, treatment using the standard drug Pioglitazone (20 mg/kg, p,o.) recorded an impressive increase in body weight. When subjected to our strongest compound AB1, the improvement of body weight was observed more than the other two compounds AB9 and AB3, as shown in **Figure 3**.

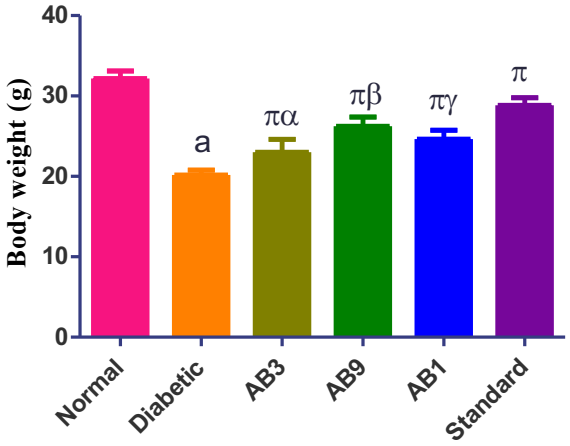

Figure 3. Effects on body weight of treatment with synthesized compounds AB1, AB9, and AB3 against streptozotocin-induced diabetes in mice. Values were expressed as mean ± SEM with n= 6. Data were analysed by using the two-way ANOVA, followed by the Bonferroni post-hoc test ($P < 0.0001$).

Blood Glucose level:

This study's results showed that the magnitude of blood glucose level in diabetic control was significantly enhanced when compared to that of normal control, $^{a}p <$

0.0001. A decrease in the level of blood glucose was observed more in the treatment with the test drugs as compared to the standard drug. Test drug AB1 demonstrated a significant decrease in the level of glucose and was more active than the standard drug. The other two compounds (AB9 and AB3) also exhibited improved ability to lower blood glucose levels as presented in **Figure 4**.

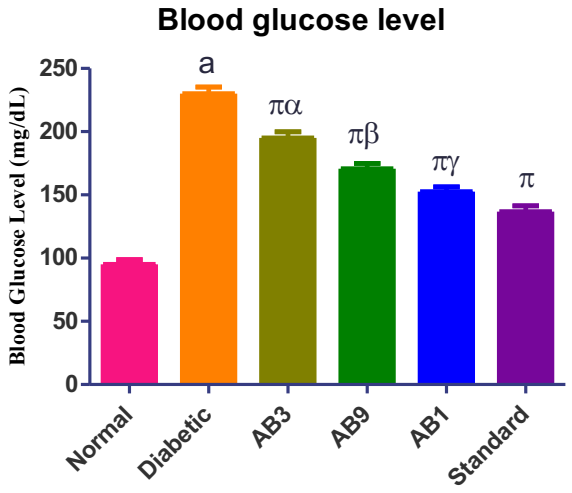

Figure 4. Effects on blood glucose level of synthesized compounds AB1, AB9 and AB3 against streptozotocin-induced diabetes in mice. Values are expressed as mean ± SEM with n = 6. Data were analysed by using the two-way ANOVA, followed by the Bonferroni post-hoc test ($P < 0.0001$).

7.4.2. Oral Glucose Tolerance Test (OGTT)

The OGTT experiment was conducted on the 15th day of protocol. Blood glucose level was monitored at different times, including 0, 15, 30, 60 and 120 minutes of glucose administration. Tolerability of glucose was also observed to be considerably reduced in the diabetic group as compared to the normal group ($^aP < 0.05$). AB1 (20 mg/kg) and Pioglitazone (20mg/kg) were shown to be the most effective in reducing BGL and similar to compound AB9 and AB3 (20 mg/kg) at 60 min and 120 min, respectively, as demonstrated in **Figure 5**.

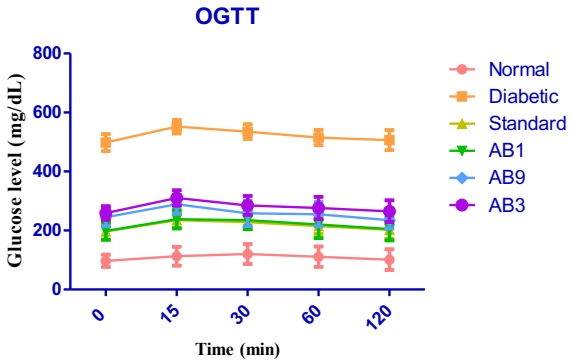

Figure 5: Oral glucose tolerance test of AB1, AB9, and AB3 in streptozotocin-nicotinamide (STZ-NA) induced diabetic mice. Values are expressed as Mean ± SD (n=6); $p < 0.0001$, when compared to the diabetic group at all time intervals; two-way ANOVA followed by Bonferroni's multiple comparison test.

7.4.4. Measurement of Lipid Profile

The test was accompanied by the taking of animal serum to investigate the lipid profile. As seen, the general level of TG, TC, and LDL was very high, and the level of HDL was very low in the diabetic group compared to the normal group ($^ap < 0.05$), as shown in **Figure 6**. Nonetheless, Pioglitazone and synthesized compounds AB1 are better in treating and lowering the levels of cholesterol, Triglycerides and LDL. Interestingly, these compounds increase the degree of HDL in mice.

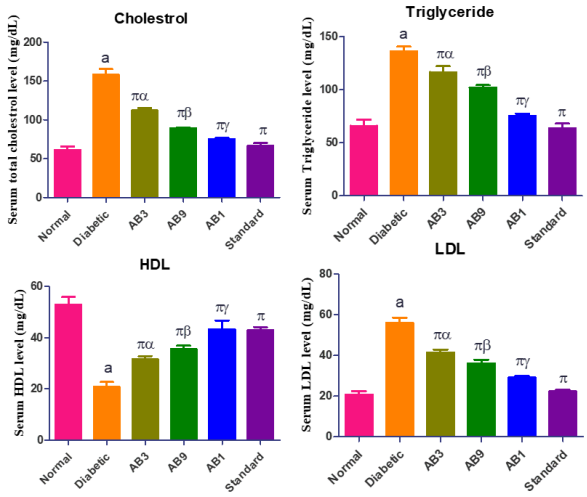

Figure 6: (a) Effects on serum total cholesterol, **(b)** serum triglyceride level, **(c)** serum HDL, and **(d)** serum LDL, of synthesised compounds AB1, AB9 and AB3. Values are expressed as mean ± SEM with n = 6. Data were analysed by using the one-way ANOVA, followed

by the Newman-Keuls multiple comparison test ($P < 0.05$).

Docking Studies:

The docking score indicates the binding free energy of the ligand-receptor complex; the smaller the docking score, the stronger the interaction is predicted. AB9 recorded the highest score in the docking score (-4.784 kcal/mol), indicating that this compound could have good binding affinity to the PTP-1B active site. Compound AB3 also displayed a favourable docking score (-4.303 kcal/mol), which is also consistent with its strong PTP-1B inhibition. The reference drug, Pioglitazone, had a docking score of -3.435 kcal/mol, which is not as favourable as compared to both AB9 and AB3, which indicated again the higher binding potential of the two novel derivatives. The docking scores indicated that the two test compounds are binding at the same site as Pioglitazone with varying modes and affinity. Compound AB9 mainly forms hydrogen bonds with ARG47, and this interaction is similar to one of the important contacts of Pioglitazone. The interaction profile of compound AB3 is more detailed with the formation of hydrogen bonds (ARG254).

Table 4. Docking scores of synthesized compounds

Compounds	Docking scores (kcal/mol)	Interactions
AB9	-4.784	ARG47
AB3	-4.303	ARG254
AB5	-4.24	ARG24, TYR46
AB1	-4.176	ARG47
AB6	-4.097	
AB4	-3.178	ARG254, GLY259, PHE182
AB2	-2.781	PHE182
AB7	-2.458	ARG47, ASP48, LYS116
AB8	-1.936	PHE182
AB10	-1.907	
Pioglitazone	-3.435	ARG47, ASP48, PHE182

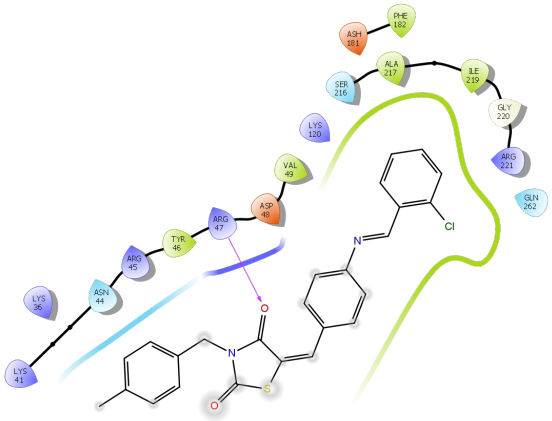

Figure 7. Docking interactions of AB9 with **PTP-1B** (PDB-ID: 1C83) with docking score -4.784 kcal/mol

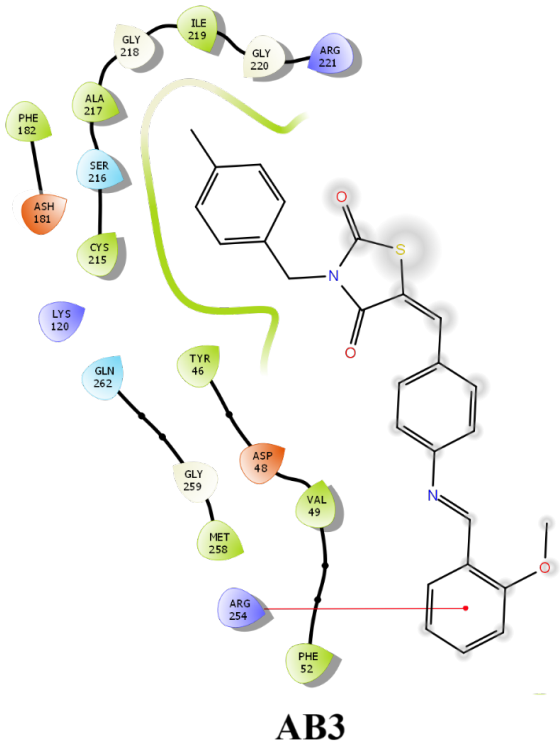

Figure 8. Docking interactions of AB3 with **PTP-1B** (PDB ID: 1C83) with docking score -4.303kcal/mol

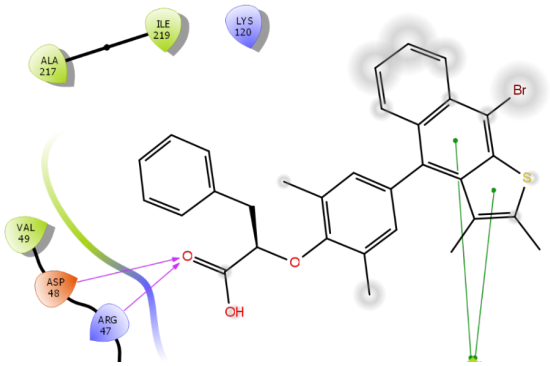

Figure 8. Docking interactions of AB3 with **PTP-1B** (PDB ID: 1C83) with docking score -3.435kcal/mol

Structure-Activity Correlation

Ten thiazolidinedione-arylidene analogues (AB1-AB10) were produced and tested as *in vitro* PTP-1B inhibitors, showing a definite correlation between strength and identity and placement of aryl substituents. Compound AB1 was the strongest inhibitor in the series, with an IC_{50} of 3.1 ± 0.29 µM, which is better than the reference inhibitor Pioglitazone (IC_{50} = 11.5 ± 0.65 µM). The high activity of AB1 has been related to the unsubstituted phenyl ring that facilitates optimum spatial orientation of the TZD scaffold to enable robust hydrogen-bonding and π-π stacking connections in the PTP1B catalytic pocket. Compounds AB9 (IC_{50}= 8.6 ± 0.37 µM) and AB3 (IC_{50}= 12.25 ± 0.46 µM) also displayed better inhibitory activity. The increased potency of AB9 may be attributed to the existence of ortho-nitro substitution, whereas the presence of the ortho-methoxy group in AB3 probably facilitates favourable polarization of the interactions and stabilize the productive binding patterns. However, the weakly electron-donating para-substitution group (AB5) exhibited only moderate inhibition (IC_{50} = 28.4 ± 0.34 µM), suggesting that para-substitution with weak electron-donating groups is not so desirable to enhance the binding of the enzymes. Derivatives AB6 (4-chloro, IC_{50} = 87.2 ± 0.55 µM), AB7 (4-bromo, IC_{50} = 52.28 ± 0.31 µM), and AB8 (2-chloro, IC_{50} = 45.3 ± 0.54 µM) had only slight improvement relative to weakly active analogues, indicating that halogen substitution adds few hydrophobic interactions to the structure, unable to generate strong PTP-1B inhibition. On the other hand, substituents with strong electron withdrawal or bulky effects in the para position, like AB4 (4-nitro, IC_{50} = 112 ± 0.15 µM) and AB10 (2,4-dichloro, IC_{50} = 130.39 ± 0.29 µM), had weak inhibitory properties. This decrease in potency could probably be attributed to steric inhibition and poor electronic influences that interfere with appropriate alignment in the active site.

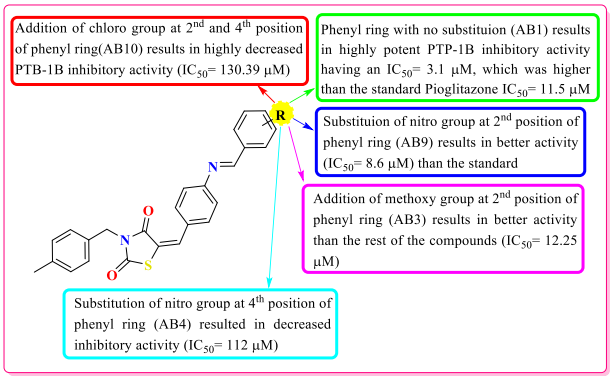

Figure 9. SAR study of TZD

In-silico ADMET prediction

The QikProp module was used to carry out in silico pharmacokinetic and drug-likeness profiling on the designed arylidene-substituted thiazolidinedione (TZD) based derivatives AB(1-10). This assessment was done consequently with the Rule of Five. Based on these criteria, a compound is said to be drug-like when it does not break more than one of the following parameters: molecular weight lower than 500 Da, calculated octanol/water partition coefficient (Log P) not exceeding ≤ 5, amount of hydrogen bond donors not exceeding ≤ 5, amount of hydrogen bond acceptors not exceeding ≤ 10. All the synthesized compounds have met the conditions of Lipinski as summarized in Figure 5.4 and have had a satisfactory molecular weight, hydrogen-bonding capability, and physicochemical characteristics. Despite moderately high Log P values, only one single violation was observed in each compound, which is reasonable in the case of an orally active drug candidate. The values calculated in predicted Caco-2 cell permeability showed good absorption in the intestine whereas solubility and human serum albumin binding parameters were within the recommended range implying good pharmacokinetic behaviour.

Table 5. Pharmacokinetic (ADME) properties prediction

Comp.	MW (Da)	#H-bond acceptors	#H-bond donors	QPlogPo/w	CIQPlogS	QPlogKhsa	Rule of Five	QPPCaco

AB1	412.50	4	0	6.303	-7.416	1.113	1	2257.499
AB2	426.53	4	0	6.608	-8.014	1.283	1	2193.982
AB3	442.53	4.75	0	6.388	-7.654	1.102	1	2179.206
AB4	457.50	5	0	5.533	-7.466	1.013	1	261.029
AB5	457.50	5	0	5.579	-7.323	0.996	1	329.481
AB6	442.53	4.75	0	6.348	-7.563	1.086	1	2204.23
AB7	446.95	4		6.808	-8.183	1.241	1	2257.357
AB8	491.40	4	0	6.888	-8.306	1.268	1	2258.381
AB9	446.95	4	0	6.743	-8.026	1.224	1	2266.449
AB10	481.39	4	0	7.245	-8.783	1.351	1	2268.049

4. Conclusion

The current research study was done to design, synthesize, and biologically profile a new family of arylidene-substituted thiazolidine-2,4-dione (TZD) analogues AB(1-10) as possible Protein Tyrosine Phosphatase 1B (PTP-1B) inhibitors on type 2 diabetes mellitus (Tsir's2DM) management. The research was premised on the fact that PTP-1B inhibition leads to an increase in insulin receptor phosphorylation, and increases in insulin sensitivity, which constitutes a promising approach to hyperglycaemia management in T2DM. Ten new derivatives of thiazolidine-2,4-dione containing various electron donor and electron withdrawing groups on the aryl ring were synthesized to determine their association between the structure and the activity (SAR). The *in vitro* PTP-1B inhibition test has shown that a variety of compounds synthesized had strong potent enzyme inhibition, with compound AB1 the most active (IC_{50}= 3.1± 0.29 μM) and the standard Pioglitazone (IC_{50}= 11.5 ± 0.65 μM). Other derivatives such as AB9 (IC_{50} = 8.6 ±0.37 0M) and AB3 (IC_{50} = 12.25 ± 0.46 0M) also showed a high degree of inhibition, meaning that the character and location of substituents on the aryl ring have a significant effect on the binding affinity and inhibition potential. The interaction profiles of the synthesized compounds in the PTP-1B active site (PDB ID: 1C83) were determined by molecular docking studies. The docking findings were consistent with experimental data and revealed that the most active compounds, especially AB1 and AB9, formed strong hydrogen bonding and π- π stacking with the main amino acid residues, i.e. Arg47, Asp48, Phe182 and Tyr46, which is the key to inhibitory activity. The docking scores also supported the binding efficiency and selectivity of the compounds to PTP-1B. The *in vivo* results showed that compounds AB1, AB3, and AB9 had significant effects on reducing the levels of fasting blood glucose, improving the body weight, and normalizing the serum lipid levels (lowering total cholesterol, triglycerides, and LDL levels and increasing the levels of HDL). These outcomes were either similar or superior to the reference drug Pioglitazone and it means that the glucose homeostasis was significantly improved. The oral glucose tolerance test (OGTT) also supported the capacity of such compounds to increase the use of glucose and insulin sensitivity. QikProp module of the Schrodinger suite in silico ADMET predictions showed that all synthesized derivatives were found to obey the Rule of Five with respect to good oral bioavailability, optimum lipophilicity (log P), acceptable molecular weights and favourable balance of donor and acceptor hydrogen bonds. The estimated values of Caco-2 permeability were indicative of acceptable intestinal absorption, and no compound had toxicity warnings or the breaking of major pharmacokinetic parameters. In summary, the carefully crafted arylidene-substituted thiazolidine-2,4-dione derivatives exhibited strong and selective PTP-1B inhibition, with compounds AB1, AB3, and AB9 displaying exceptional in vitro, in vivo, and in silico antidiabetic characteristics. These results emphasize TZD-derived scaffolds, especially AB1, as encouraging lead candidates for additional advancement in treating type 2 diabetes mellitus.

References

1. Hossain, M. J., Al-Mamun, M., & Islam, M. R. (2024). Diabetes mellitus, the fastest growing global public health concern: Early detection should be focused. *Health science reports*, *7*(3), e2004. https://doi.org/10.1002/hsr2.2004
2. Kumar, A., Gangwar, R., Ahmad Zargar, A., Kumar, R., & Sharma, A. (2024). Prevalence of diabetes in India: A review of IDF diabetes atlas 10th edition. *Current diabetes reviews*, *20*(1), 105-114. https://doi.org/10.2174/1573399819666230413094200
3. Kaul, K., Tarr, J. M., Ahmad, S. I., Kohner, E. M., & Chibber, R. (2012). Introduction to diabetes mellitus. *Diabetes: an old disease, a new insight*, 1-11. https://doi.org/10.1007/978-1-4614-5441-0_1
4. Dilworth, L., Facey, A., & Omoruyi, F. (2021). Diabetes mellitus and its metabolic complications: the role of adipose tissues. *International journal of molecular sciences*, *22*(14), 7644. https://doi.org/10.3390/ijms22147644
5. Iheagwam, F. N., & Iheagwam, O. T. (2025). Diabetes mellitus: The pathophysiology as a canvas for management elucidation and strategies. *Medicine in Novel Technology and Devices*, *25*, 100351. https://doi.org/10.1016/j.medntd.2025.100351
6. Sun, Y., Dinenno, F. A., Tang, P., & Kontaridis, M. I. (2024). Protein tyrosine phosphatase 1B in metabolic and cardiovascular diseases: From mechanisms to therapeutics. *Frontiers in Cardiovascular Medicine*, *11*, 1445739. https://doi.org/10.3389/fcvm.2024.1445739
7. Haider, A. S., Ambatwar, R., & Khatik, G. L. (2025). Insights into PTP1B inhibitors as antidiabetic agents: Current research and future perspectives. *European Journal of Medicinal Chemistry*, *295*, 117791. https://doi.org/10.1016/j.ejmech.2025.117791
8. Liu, Z., Gao, H., Zhao, Z., Huang, M., Wang, S., & Zhan, J. (2023). Status of research on natural protein tyrosine phosphatase 1B inhibitors as potential antidiabetic agents: Update. Biomedicine & Pharmacotherapy, 157, 113990. https://doi.org/10.1016/j.biopha.2022.113990
9. Norris, K., Norris, F., Kono, D. H., Vestergaard, H., Pedersen, O., Theofilopoulos, A. N., & Møller, N. P. H. (1997). Expression of protein-tyrosine phosphatases in the major insulin target tissues. *FEBS letters*, *415*(3), 243-248. https://doi.org/10.1016/S0014-5793(97)01133-2
10. Behl, T., Gupta, A., Sehgal, A., Albarrati, A., Albratty, M., Meraya, A. M., ... & Bungau, S. (2022). Exploring protein tyrosine phosphatases (PTP) and PTP-1B inhibitors in management of diabetes mellitus. *Biomedicine & Pharmacotherapy*, *153*, 113405. https://doi.org/10.1016/j.biopha.2022.113405
11. Bourebaba, L., Serwotka-Suszczak, A., Bourebaba, N., Zyzak, M., & Marycz, K. (2023). The PTP1B inhibitor trodusquemine (MSI-1436) improves glucose uptake in equine metabolic syndrome affected liver through anti-inflammatory and antifibrotic activity. *International Journal of Inflammation*, *2023*(1), 3803056. https://doi.org/10.1155/2023/3803056
12. Hua, X., Xu, M., Yang, M., Zhang, Y., Ma, J., Cheng, L., ... & Guo, M. (2025). Hypoglycemic and hypolipidemic bioactive compounds from edible traditional Chinese medicines and their action of mechanisms explored by multitarget affinity ultrafiltration with liquid chromatography–mass spectrometry. *Food Frontiers*, *6*(1), 65-85. https://doi.org/10.1002/fft2.488
13. Behl, T., Gupta, A., Albratty, M., Najmi, A., Meraya, A. M., Alhazmi, H. A., ... & Bungau, S. G. (2022). Alkaloidal phytoconstituents for diabetes management: exploring the unrevealed potential. *Molecules*, *27*(18), 5851. https://doi.org/10.3390/molecules27185851
14. Long, N., Le Gresley, A., & Wren, S. P. (2021). Thiazolidinediones: an in–depth study of their synthesis and application to medicinal chemistry in the treatment of diabetes mellitus. *ChemMedChem*, *16*(11), 1717-1736. https://doi.org/10.1002/cmdc.202100177
15. Gautam, P., Bisht, P., Gautam, A., Gupta, G. D., Singh, R., & Verma, S. K. (2023). A comprehension on structure guided alignment dependent 3D-QSAR modelling, and molecular dynamics simulation on 2, 4-thiazolidinediones

as aldose reductase inhibitors for the management of diabetic complications. *Journal of Biomolecular Structure and Dynamics*, 1-20. https://doi.org/10.1080/07391102.2023.2275190

16. Bhattarai, B. R., Kafle, B., Hwang, J. S., Khadka, D., Lee, S. M., Kang, J. S., ... & Cho, H. (2009). Thiazolidinedione derivatives as PTP1B inhibitors with antihyperglycemic and antiobesity effects. *Bioorganic & medicinal chemistry letters*, *19*(21), 6161-6165. https://doi.org/10.1016/j.bmcl.2009.09.020
17. Bhattarai, B. R., Kafle, B., Hwang, J. S., Ham, S. W., Lee, K. H., Park, H., ... & Cho, H. (2010). Novel thiazolidinedione derivatives with anti-obesity effects: dual action as PTP1B inhibitors and PPAR-γ activators. *Bioorganic & Medicinal Chemistry Letters*, *20*(22), 6758-6763. https://doi.org/10.1016/j.bmcl.2010.08.130
18. Wang, W., Zhou, X., Kwong, J. S., Li, L., Li, Y., & Sun, X. (2017). Efficacy and safety of thiazolidinediones in diabetes patients with renal impairment: a systematic review and meta-analysis. *Scientific reports*, *7*(1), 1717.Wang, W., Zhou, X., Kwong, J. S., Li, L., Li, Y., & Sun, X. (2017). Efficacy and safety of thiazolidinediones in diabetes patients with renal impairment: a systematic review and meta-analysis. *Scientific reports*, *7*(1), 1717. https://doi.org/10.1038/s41598-017-01965-0
19. Hussain, F., Khan, Z., Jan, M. S., Ahmad, S., Ahmad, A., Rashid, U., ... & Sadiq, A. (2019). Synthesis, in-vitro α-glucosidase inhibition, antioxidant, in-vivo antidiabetic and molecular docking studies of pyrrolidine-2, 5-dione and thiazolidine-2, 4-dione derivatives. *Bioorganic chemistry*, *91*, 103128. https://doi.org/10.1016/j.bioorg.2019.103128
20. Huneif, M. A., Alshehri, D. B., Alshaibari, K. S., Dammaj, M. Z., Mahnashi, M. H., Majid, S. U., ... & Sadiq, A. (2022). Design, synthesis and bioevaluation of new vanillin hybrid as multitarget inhibitor of α-glucosidase, α-amylase, PTP-1B and DPP4 for the treatment of type-II diabetes. *Biomedicine & Pharmacotherapy*, *150*, 113038. https://doi.org/10.1016/j.biopha.2022.113038
21. Liu, S. Y., Yu, L. J., Zhang, S. N., Yue, J. K., Jiang, G. J., Lu, S. H., ... & Huang, G. H. (2025). Isoquercitrin Improves Insulin Resistance by Inhibiting PTP1B-Regulated IRS/PI3K/AKT Signaling Pathway. *Chinese Journal of Integrative Medicine*, 1-10. https://doi.org/10.1007/s11655-025-3934-6
22. Peter, J. A., Olatunde, A., Aminu, S., Umar, I. A., & Mohammed, A. (2022). Effects of p-Hydroxybenzaldehyde, Vanillin, and Syringaldehyde on Protein Tyrosine Phosphatase 1B Activity. *Current Enzyme Inhibition*, *18*(3), 194-199. https://doi.org/10.2174/1573408018666220630140400
23. Naeem, F., Aqeel, M., Zahid, M. A., Babar, M. M., Shah, F. A., Agouni, A., & Malik, S. Z. (2025). The effects of ondansetron on diabetes and high-fat diet-induced liver disease: a critical role for protein tyrosine phosphatase 1B. *Frontiers in pharmacology*, *16*, 1565628. https://doi.org/10.3389/fphar.2025.1565628
24. Zhao, Y., Liu, Y., Deng, J., Zhu, C., Ma, X., Jiang, M., & Fan, D. (2023). Ginsenoside F4 alleviates skeletal muscle insulin resistance by regulating PTP1B in type II diabetes mellitus. *Journal of Agricultural and Food Chemistry*, *71*(39), 14263-14275. https://doi.org/10.1021/acs.jafc.3c01262
25. Kanda, J., Izumo, N., Kobayashi, Y., Onodera, K., Shimakura, T., Yamamoto, N., ... & Wakabayashi, H. (2017). Effect of the antidiabetic agent pioglitazone on bone metabolism in rats. *Journal of pharmacological sciences*, *135*(1), 22-28. https://doi.org/10.1016/j.jphs.2017.08.004
26. Kausar, M. A., Parveen, K., Siddiqui, W. A., Anwar, S., Zahra, A., Ali, A., ... & Saeed, M. (2021). Nephroprotective effects of polyherbal extract via attenuation of the severity of kidney dysfunction and oxidative damage in the diabetic experimental model. *Cellular and Molecular Biology*, *67*(4), 42-55. https://doi.org/10.14715/cmb/2021.67.4.6
27. Okoduwa, S. I. R., Umar, I. A., James, D. B., & Inuwa, H. M. (2017). Appropriate insulin level in selecting fortified diet-fed, streptozotocin-treated rat model of type 2 diabetes for anti-

diabetic studies. *PLoS One*, *12*(1), e0170971. https://doi.org/10.1371/journal.pone.0170971

28. Gao, X., Xie, Q., Kong, P., Liu, L., Sun, S., Xiong, B., ... & Xiang, H. (2018). Polyphenol- and caffeine-rich postfermented pu-erh tea improves diet-induced metabolic syndrome by remodeling intestinal homeostasis in mice. *Infection and Immunity*, *86*(1), 10-1128. https://doi.org/10.1128/iai.00601-17
29. Li, T. T., Wan, Q., Zhang, X., Xiao, Y., Sun, L. Y., Zhang, Y. R., ... & Yang, W. C. (2022). Stellate ganglion block reduces inflammation and improves neurological function in diabetic rats during ischemic stroke. *Neural Regeneration Research*, *17*(9), 1991-1997. https://doi.org/10.4103/1673-5374.335162
30. McDowell, R. E., Barabas, P., Augustine, J., Chevallier, O., McCarron, P., Chen, M., ... & Curtis, T. M. (2018). Müller glial dysfunction during diabetic retinopathy in rats is reduced by the acrolein-scavenging drug, 2-hydrazino-4, 6-dimethylpyrimidine. *Diabetologia*, *61*(12), 2654-2667. https://doi.org/10.1007/s00125-018-4707-y
31. Winzell, M. S., & Ahrén, B. (2004). The high-fat diet–fed mouse: a model for studying mechanisms and treatment of impaired glucose tolerance and type 2 diabetes. *Diabetes*, *53*(suppl_3), S215-S219. https://doi.org/10.2337/diabetes.53.suppl_3.S215
32. Nagy, C., & Einwallner, E. (2018). Study of in vivo glucose metabolism in high-fat diet-fed mice using oral glucose tolerance test (OGTT) and insulin tolerance test (ITT). *Journal of visualized experiments: JoVE*, (131), 56672. https://doi.org/10.3791/56672
33. Raza, I., Sohail, A., Muneer, H., Fayyaz, H., Uddin, Z., Almars, A. I., ... & Ullah, I. (2024). Viscosol Treatment Ameliorates Insulin-Mediated Regulation of Dyslipidemia, Hepatic Steatosis, and Lipid Metabolism by Targeting PTP1B in Type-2 Diabetic Mice Model. *International Journal of Endocrinology*, *2024*(1), 3914332. https://doi.org/10.1155/ije/3914332
34. Wang, C. D., Teng, B. S., He, Y. M., Wu, J. S., Pan, D., Pan, L. F., ... & Zhou, P. (2012). Effect of a novel proteoglycan PTP1B inhibitor from Ganoderma lucidum on the amelioration of hyperglycaemia and dyslipidaemia in db/db mice. *British Journal of Nutrition*, *108*(11), 2014-2025. https://doi.org/10.1017/S0007114512000153
35. Nandi, S., & Saxena, M. (2020). Potential inhibitors of protein tyrosine phosphatase (PTP1B) enzyme: promising target for type-II diabetes mellitus. *Current Topics in Medicinal Chemistry*, *20*(29), 2692-2707. https://doi.org/10.2174/1568026620999200904121432
36. Varshney, K., Gupta, A. K., Rawat, A., Srivastava, R., Mishra, A., Saxena, M., ... & Saxena, A. K. (2019). Synthesis, SAR and docking studies of substituted aryl phenylthiazolyl phenylcarboxamide as potential protein tyrosine phosphatase 1B (PTP 1B) inhibitors. *Chemical Biology & Drug Design*, *94*(1), 1378-1389. https://doi.org/10.1111/cbdd.13515
37. Thareja, S., Verma, S. K., Haksar, D., Bhardwaj, T. R., & Kumar, M. (2016). Discovery of novel cinnamylidene-thiazolidinedione derivatives as PTP-1B inhibitors for the management of type 2 diabetes. *RSC advances*, *6*(110), 108928-108940. https://doi.org/10.1039/C6RA24501C
38. Ojo, O. A., Adegboyega, A. E., Johnson, G. I., Umedum, N. L., Onuh, K., Adeduro, M. N., ... & Johnson, T. O. (2021). Deciphering the interactions of compounds from Allium sativum targeted towards identification of novel PTP 1B inhibitors in diabetes treatment: a computational approach. *Informatics in Medicine Unlocked*, *26*, 100719. https://doi.org/10.1016/j.imu.2021.100719
39. Saeed, M., Shoaib, A., Tasleem, M., Alabdallah, N. M., Alam, M. J., Asmar, Z. E., ... & Badraoui, R. (2021). Assessment of antidiabetic activity of the shikonin by allosteric inhibition of protein-tyrosine phosphatase 1B (PTP1B) using state of art: an in silico and in vitro tactics. *Molecules*, *26*(13), 3996. https://doi.org/10.3390/molecules26133996